Iranica Journal of Energy & Environment
Journal Homepage: www.ijee.net
IJEE an official peer review journal of Babol Noshirvani University of Technology, ISSN:2079-2115

Effect of Stall Delay Model on Momentum Distribution of Wind Turbine's Blade under Yaw Condition: Compared to MEXICO Experiment

A. Khanjari[1,*], E. Mahmoodi [2] , A. Sarreshtehdari[1] and M. Kordi[2]

[1]*Department of Mechanical Engineering, Shahrood University of Technology, Shahrood, Iran*
[2]*Department of Mechanical Engineering of Biosystems, Shahrood University of Technology, Shahrood, Iran*

P A P E R I N F O

Paper history:
Received 11 March 2018
Accepted in revised form 11 April 2018

Keywords:
Wind turbine
Yaw angel
Blade element momentum theory
3D correction

A B S T R A C T

In this paper, the effect of stall delay on distribution of normal forces in different sections of rotor are studied by an enhanced version of the blade element momentum theory (BEM), based on the 3D correction Chaviaropoulos and Hansen mode. This model is computed at wind speed of 24m/s under the yaw angle 15◦. It is found that the BEM calculation on the outer (the radial distance more than 35% spanwies) spanwise is more trustable than inner spanwise. At 60, 82 and 92% spans, the 3D correction does not affect the output result and stall does not occur. Relative velocity rose dramatically at 25 and 35% spans, consequently angle of attack increased too particularly between azimuth angles from 270◦ up to 90◦. In this regions, stall phenomena are happened. Also it is found that the 3D correction has the maximum effect on 35 and 25% spans. The maximum improvement is 99.57% at 35% section and the azimuth angle 121◦.

***doi**: 10.5829/ijee.2018.09.01.03*

Nomenclature

a	Normal induction factor	Greek letters	
a'	Tangential induction factor	φ	Flow angle (rad)
v	Velocity(m/s)	φ_y	Yaw angle
W	Work (J)	β	Pitch angle (rad)
C_l	Lift coefficient	ρ	Density (kg/m^3)
C_d	Drag coefficient	Ω	Rotor speed (rad/s)
F	Force (N)	σ'	Solidity
c	Chord (m)	θ	Azimuth angle
r	Radius (m)	ΔC_l	Difference between 2D and 3D lift coefficient
P	Pressure (kPa)		
f	Prandtl's tip loss factor		

INTRODUCTION

In recent years, study of mathematical models applied to horizontal wind turbine has become significant due to increasing use of wind energy demand. On the other hand, predicting the blades loads accurately is one of the most important parts of calculation in wind turbine aerodynamics. Corrected versions of the classical BEM theory as one of the fast and trustable model in wind turbine design is still used by researchers to predict wind turbine performance [1-4]. The airfoil characteristics are mostly based on 2D wind tunnel measurements. Due to 3D effects, a BEM code using airfoil data obtained directly from 2D wind tunnel measurements will not yield the correct loading and power [5].

Some researchers studied the BEM code to promote more accurate results. Mahmoodi showed that at high wind speed, improved BEM model predicts more accurate than CFD models (actuator disc model) in none yaw condition [6]. However, a lot of efforts have been done in order to make BEM more trustable by taking to account some corrections which affected the stall in wind aerodynamic.

To overcome the impossibility of describing inside of the one-dimensional (1D) code, the three-dimensional (3D) radial flow along the blades was proposed by Lanzafame and Messina [7]. This interpolation overestimated the 2D lift coefficient in the fully stalled region, which led to possible consideration of the radial flow inside a 1D BEM code [7]. The effect of 3D correction on the centrifugal pumping effect, which

* Corresponding author: Ali khanjari
E-mail: ali_khanjari69@yahoo.com

postpones the separation point along the airfoil surface on MEXICO wind turbine at none yaw flow, was performed by enhanced BEM model [8]. The aerodynamic loads on wind turbine's blades are widely fluctuated when yaw flow happens. Therefore, it is important to evaluate 3D corrections in yaw flow.

Li Q shows that in the case of the yaw angle of $\phi = 30°$, the power coefficients showed larger values than those of $\phi = 0°$ at the low tip speed ratio ranges of $1.5 < \lambda < 2.5$ [9]. Bouatem and Mers showed the BEM code in yaw condition by using the 3D correction could have a satisfactory result to predict the normal force on wind turbine [10]. But there are some questions about the effect of 3D correction at yaw flow. For example, in which sections of blade rotor, could be 3D correction used for improving normal force distribution? How much could 3D correction improve normal force distribution on different span at yaw flow?

In this work, it will be shown that how Chaviaro Poulos and Hansen 3D correction can modify the normal force distribution in different sections of rotor and azimuth angle based on enhanced BEM code in experimental model controlled condition (MEXICO) wind turbine at yaw flow.

MATERIAL AND METHODS

The measurements from the MEXICO experiment are employed to validate the computations in this study. The MEXICO experiment is an EU project with the main goal of providing a database of aerodynamic measurements for a wind turbine model. In this international effort, an extensively instrumented wind turbine model has been tested in the large scale low speed facility (LLF) of the Germany Dutch wind tunnel (DNW), under several flow conditions [11, 12]. The MEXICO wind turbine blade is comprised of three different airfoil sections; a DU 91-W2-250 in the root region; a RISOA1-21 at mid span sections and a NACA 64-418 nearing the tip of the blade (see Fig. 1).

The BEM theory

The basic tool to find out wind turbine's aerodynamics is the blade element momentum theory in which the flow is assumed to be inviscid, incompressible and axisymmetric [13]. The basis of the BEM model that is employed in this research was developed by Glauert and described in detail by Hansen [8, 14, 15]. In this theory, the blade is divided into several elements and the study is conducted element by element. The performance of each blade element is deduced by applying the principle of momentum conservation [16, 17].

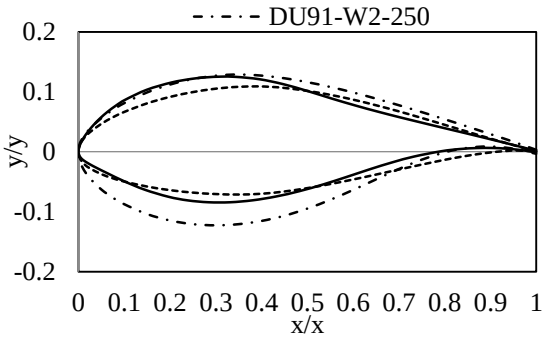

Figure 1. Geometry of three airfoils that use in the MEXICO wind turbine blade

The experience shows that a wind turbine generates a wake downstream of the rotor [18, 19]. This wake has a significant impact on the flow upstream. Indeed, the wind speed just before the rotor V_2 is slowed down by the wake induced velocity. By applying the theorem of momentum in the normal direction, [18, 19], is obtained:.

$$V_2 = V_1(1 - a) \tag{1}$$

where a is the normal induction factor. In this case, a correction as Equation (2) described in [20] was used to avoid the breaking down of the integration process. Parameter k is an auxiliary function described in Equation (2) and $a_c = 0.3$ is the separation point of the thrust coefficient in the high normal induction factor:

$$a = \begin{cases} (k+1)^{-1}, & a \le a_c \\ \frac{1}{2}(2 + k(1-2a_c) - \sqrt{(k(1-2a_c)+2)^2 + 4(k.{a_c}^2 - 1)}), & a \ge a_c \end{cases} \tag{2}$$

$$k = \frac{4f sin\phi^2}{\acute{\sigma}(c_l \cos(\phi) + c_d \sin(\phi))} \tag{3}$$

where C_l is the lift coefficient, C_d is the drag coefficient. The second enhancement on the BEM method is tip loss correction. In this case, f is Prandtl's tip loss factor, Equation (4) correct the turbine as a finite bladed rotor.

$$f = \frac{2}{\pi} arcos(e^{-\left(\frac{3(R-r)}{2rsin\phi}\right)}) \tag{4}$$

$$\acute{\sigma} = 3c/2\pi r \tag{5}$$

A Similar relation for the rotational speed is defined as follows, which is called a tangential induction factor, a' [18, 19].

$$a' = \frac{w_{i2}}{\Omega} \tag{6}$$

where w_{i2} is the tangential induced velocity at the plane just before the rotor and $\acute{a}$ is the tangential induction factor.

$$\phi = atan\left(\frac{V_1(1-a)}{r\Omega(1+\acute{a})}\right) \tag{7}$$

$$\alpha = \phi - \beta \quad (8)$$

where ϕ is the angle of flow and α is the angle of attack. As illustrated in Fig. 2, the normal and tangential aerodynamic forces could be calculated using the aerodynamic coefficients, the angle of flow and the angle of attack of the profile. The partial normal force (normal to the rotor plane) is given by the following equation [18, 19]:

$$dF_a = \frac{1}{2}\rho v^2[c_l\cos(\phi) + c_d\sin(\phi)]c(r)dr \quad (9)$$

Modeling under yaw condition

The wind turbine will operate under yaw conditions when the wind direction is not perpendicular to the rotor plane. As a result, the blades are not subject to the same conditions, the blade load, the induced velocities and the angle of attack varies depending on the azimuthal position (Fig. 3).

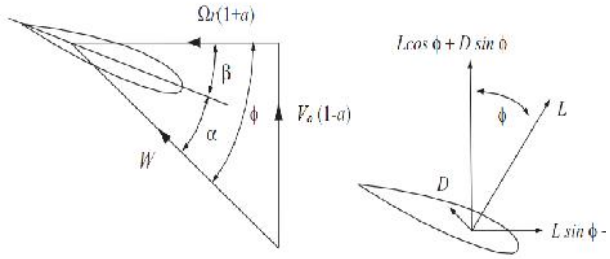

Figure 2. Arrangement of how to analysis a blade element.

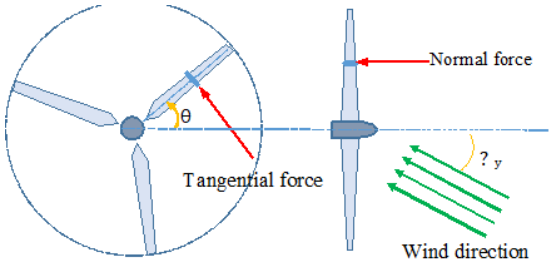

Figure 3. Wind direction and normal and tangential force direction in yaw condition.

Accordingly, the angle of attack is calculated by using Equation (10).

$$\phi = \text{atan}\left(\frac{V_1\cos(\phi_y)(1-a)}{[r\Omega - v_1\sin(\theta)\cos(\phi_y)](1+\acute{a})}\right) \quad (10)$$

Skewed wake correction

In yaw conditions, the wind turbine wake is not aligned to the rotor axis. However, the blade element momentum theory is originally developed for axisymmetric flow. The BEM model needs to be corrected to take this skewed wake effect into account. In this work the correction proposed by literature [18, 19] is used:

$$a_{cor} = a[1 + \frac{15}{35}\frac{r}{R}\tan\left(\frac{\phi_y}{2}\right)\cos(\theta)] \quad (11)$$

3D modeling for the stall region

The analytical code based on the BEM theory is an 1D code, and it is not able to take into account the 3D flows along the wind turbine blades. The radial flow along the blade postpones the separation point along the airfoil surface (Himmelskamp effect). Therefore, some models are developed by researchers for the inclusion of this effect inside the BEM codes. By developing new interpolations on the aerodynamic coefficients of airfoils, a reliable agreement is gained in the blade stall state [7, 21, 22]. An airfoil data correction described by literature [23] model was used in the present work to convert lift data from two dimensions to three dimensions and so the inclusion of the Himmelskamp effect.

$$C_{l,3D} = C_{l,2D} + x\left(\frac{c}{r}\right)^y\cos^4(\phi)(C_{l,inv} - C_{l,2D}) \quad (12)$$

Fig. 4 describes how to reproduce the lift coefficients. The linear part of the curve (inviscid part) is extended to cover the stall region. The difference between two curves $\Delta Cl = Cl,\text{inv} - Cl,2D$ is multiplied by $x(c/r)y$, where x and y are 2.2 and 1, respectively, according to the literature [24](Breton, 2008), and c/r is the local division of the chord (c) by the radius value. Actually, it is added to the original airfoil data (OAD) to result in the modified airfoil data (MAD) in an angle of attack (AOA) (α) range of validity from −15◦ to 45◦.

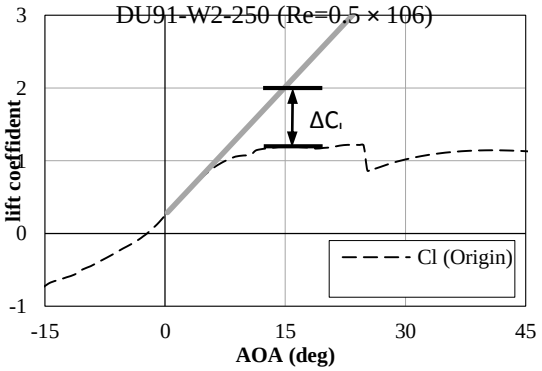

Figure 4. The preparation of lift coefficients for 3D conversion.

Methodology

In this paper, following steps are taken to get the final results:

1. Normal force in different sections of blade is computed by corrected version of the BEM model in yaw condition.
2. The results of normal force based on BEM model in step 1 are compared to the experimental measurements and other three results of studies in this wind turbine to validate the BEM model.
3. Distributions of normal force and angel of attack are shown by polar contour.

4. Effects of ΔC_l and angle of attack on normal force distribution on the blade in yaw angle are discussed.

A code was developed for the solution of the algorithm illustrated in Fig. 5, considering different yaw angle. A GNU Complier Collection (GCC) was used as the calculation engine, whereas TXT files were used to facilitate data input and output. GCC/TXT interfacing was performed in an automated manner.

RESULTS AND DISCUSSION

The results of this study are compared with the other three studies in MEXICO wind turbine. These three studies in MEXICO wind turbine are RISØ-3DTURB, TU Delft Panel code and Technion CFD [25]. The RISØ-3DTURB is developed in co-operation between the Department of Mechanical Engineering at the Technical University of Denmark and The Department of Wind Energy at Risø National Laboratory. The EllipSys3D code is a multi-block finite volume discretization of the incompressible Reynolds Averaged Navier-Stokes (RANS) equations in general curvilinear coordinates [25].

The TU Delft Panel code used in this analysis is a potential flow free-wake panel code developed in House at TU Delft. The body and the wake are represented by source and doublet distribution which are solved for each time-step. One of the major drawbacks of this model is its limitation in stall analysis. For this reason it should be used only in attached flow conditions. Moreover, the model is a dynamic model and is hence suited for yawed flow calculations (again it is for attached conditions only, and so dynamic stall could not be modeled) [25].

The Technion CFD was carried out using STAR-CD Ver. 3.26 code. The code is based on the finite volume approach and it uses multi-block meshes which enable the prediction of flows over complex geometries. In the Technion CFD the transient, turbulent, incompressible RANS equations were solved [26]

In this study, calculations of normal force are performed at wind speed 24 m/s under yaw angle 15◦ at 25, 35, 60, 82 and 92% spans and compared with the other three studies. Figs. 6 and 7 represent the evolution of normal force as a function of the azimuth angle at 92 and 82% of the blade sections. Measured and calculated curves show the same tendencies and they are almost in same phase with experimental data. At 92% span the results of this study with a constant difference, have satisfactory trend against the experimental data than other three studies. The maximum relative error for the BEM code (MAD and OAD) span and azimuth angle 336◦were 44 and 82 % respectively. At same azimuth angle the maximum relative error for Technion CFD and RISØ-3DTURB were 40% and 42%. In these sections due to the high wind speed, effects of the boundary layer thickness in wind tunnel on wake and wind turbine rotor were reduced that it causes the calculated curves be almost in same phase against experimental data. Also in these sections stall could not happen because the difference between (OAD) and (MAD) was little.

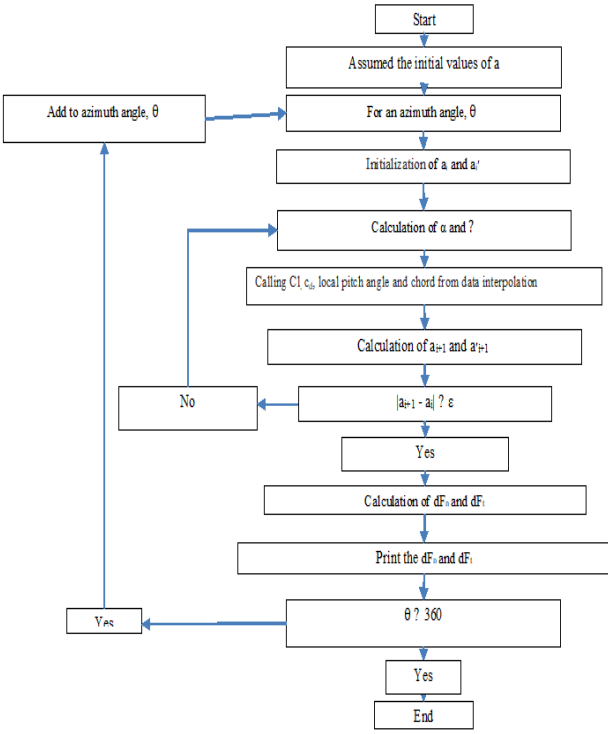

Figure 5. Algorithm designed for the enhanced BEM method in the current study

Both results of this study (OAD and MAD) have satisfactory trend against the experimental data were compared to other three studies at 60% span in Fig. 8. In Figs. 9 and 10 at 35 and 25% spans, results of BEM (MAD) code have different trend against the experimental data. The normal force of BEM (MAD) code have a considerable difference against the experimental data at 25% span. In this section, the maximum relative error for the BEM (MAD) code is 39% at the azimuth angle of 340◦ and the maximum relative error for TU Delft Panel at the azimuth angle of 0◦ is 18%. In 25 and 35% sections difference between (OAD) and (MAD) was much more than the other sections. It shows that in these sections deep stall was happened. In this study, phase of measurement is found to be different from root to tip, in which the maximum normal force at the root occurs at θ ~ 240◦ and at the tip it is shifted to θ ~ 180◦. The physical phenomena associated with this phase shift are described in literature [26] where it is explained to be a result of the variation of induced velocities over the azimuth angle. Near the tip, this variation is mainly induced by tip vortices where it is induced by root vorticity at the more inboard positions, leading to an opposite phase.

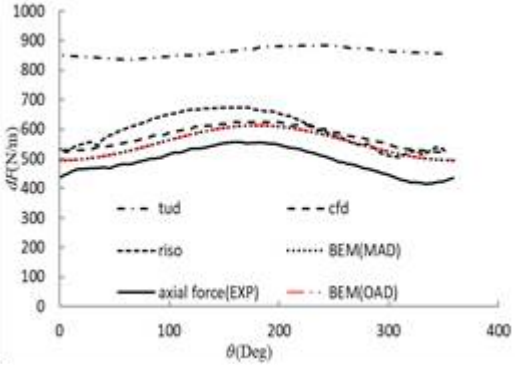

Figure 6. Normal force distribution at 92% span, for V=24m/s & ϕ_y=15◦.

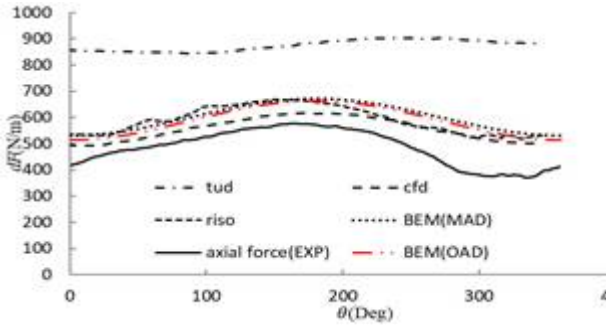

Figure 7. Normal force distribution at 82% span, for V=24m/s & ϕ_y=15◦.

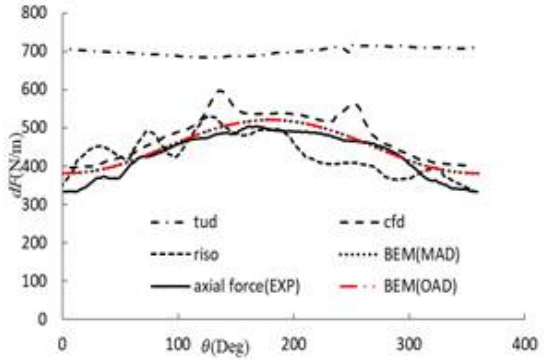

Figure 8. Normal force distribution at 60% span, for V=24m/s, & ϕ_y=15◦.

Fig. 11 shows distribution of normal force on rotor plan, semicircle between azimuthal angles from 270◦ up to 90◦ is introduced as upper half and another side is introduced as bottom half. The variation of the normal force as a function of the azimuthal angle is periodic at 92, 82, 60, 35 and 25% spans. Majority of this fluctuation at high wind speed is due to advancing and retreating effect. The advancing and retreating blades can provide stall at these sections and increase the cyclic loads. This might be an important consideration in the fatigue analysis of the blade. The presence of stall could affect the complexity of inflow distribution in the rotor plane and normal force distribution. Also at root and tip spans amount of the amplitude fluctuation in full azimuth rotation are more than mid span. The physical phenomenon is that under yawed flow, by the time that stall is occurred, radial velocity is found to increase from root to tip with some complex behavior in the root and tip spanwises at upper half [27]. Deep Stall is occurred by excessive increase of angle of attack. In the yawed flow, the angle of attack on each blade is continuously changing due to changes of wind velocity on the blade. Fig. 12, shows distribution of angle of attack on rotor plan under yaw condition. In this case, when a blade sits in upper half, it is deeper into the wake than when it sits

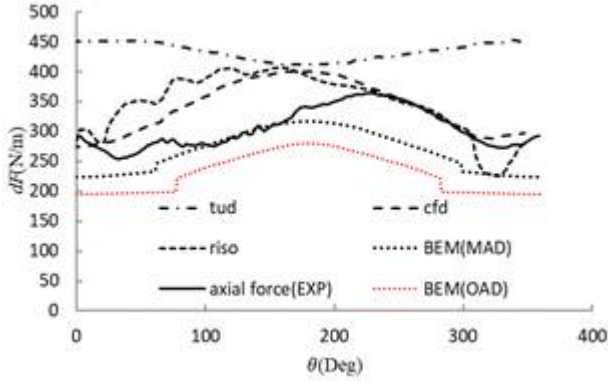

Figure 9. Normal force distribution at 35% span, for V=24m/s & ϕ_y=15◦.

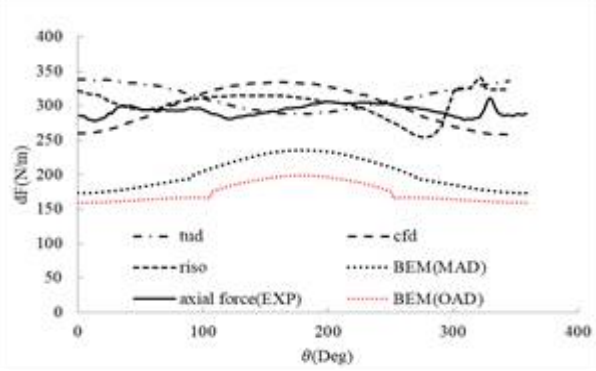

Figure 10. Normal force distribution at 25% span, for V=24m/s & ϕ_y=15◦.

in bottom half. In other words, in the bottom half, blade gains a higher wind and thus has higher aerodynamic load For wind tunnel measurements on DU91-W2-250 and RISØ A1-21airfoils at Re =5 * 10^5 and Re=1.6 * 10^6 which is within the *Re*-range for rotor measurements, stall should have been occrued at α stall = 15.8◦ for DU91-W2-250 and α stall = 9.71◦ for RISØ A1-21 because C_L dropped suddenly (Mahmoodi et al., 2013). In the yawed flow case results in Fig. 12 showed α is about 36◦ α>α stall near the root span during the entire rotational cycle especially at upper half. The rotor blades are, hence, expected to have undergone substantial dynamic stall at root spanwise.

Comparing the result between 3D correction and 2D airfoil lift can show where stall was happened.
3D correction just impacts on lift coefficient when angle of attack is heightened. Fig. 13 shows the difference between $C_{l,3D} - C_{l,2D}$. Whenever ΔC_l increases, results showed the stall has occurred. In root span 25 and 35% the value of ΔC_l is more than other spans.

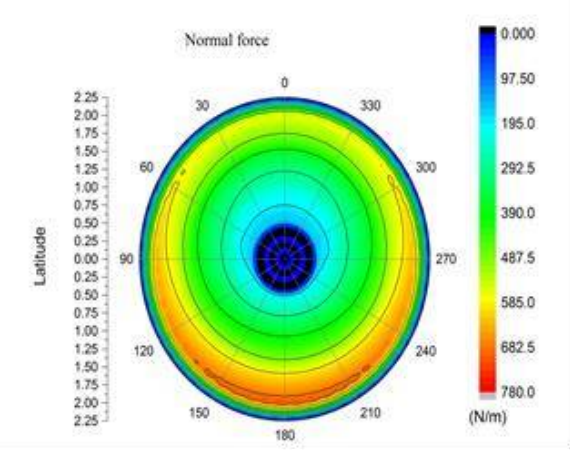

Figure 11. Normal force distribution on the rotor plan under yaw angle of 15◦.

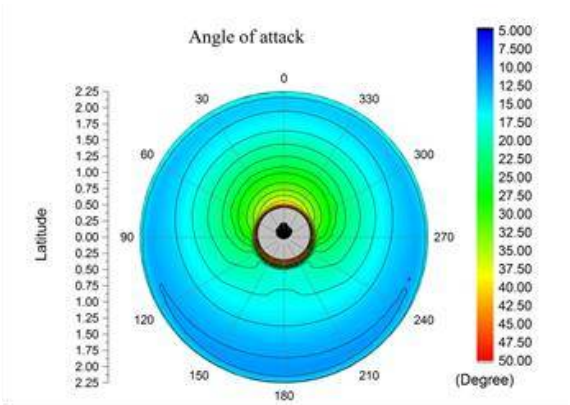

Figure 12. Distribution of angle of attack on the rotor plan under yaw angle of 15◦.

However, at tip span, where NACA foil is situated, variation of the normal force as a function of the azimuthal angle is cyclic but 3D correction does not act. In other words, stall could not happen and advancing and retreating blade can just increase the cyclic loads in this section. Mahmoodi et al. shows the 3D correction could improve 13.3 and 6.7% of the relative error for normal force in 25 and 35% sections in none yaw flow when wind turbine works in turbulent region [8]. In this study the percentage of relative error improvement for normal force in different sections are shown using the Chaviaro Poulos and Hansen 3D correction.
The percentage of improvement for the enhanced BEM model iterated with the MAD is illustrated in Fig. 14. As can be seen, the normal force has significantly affected the blade root. The improvement made where the blade is rotating between azimuths angles from 90◦ to 270◦ at 25% span. In this situation, maximum improvement is 38.43% at the azimuthal angle 159◦. This is because of decreasing *c/r* ratio in Equation (14) as the local radius is rising up more than the local chord. The 3D correction has the maximum effect on 35% span at the azimuth angle between 60˚ to 183◦. The amount of improvement at 35% span where the DU91-W2-250 airfoil is situated is more than 25% spanwise. In this section, the maximum improvement is 99.57% at the azimuth angle 121˚. It is shown when blade sits in bottom half, 3D correction has a good performance. This is due to the increase of local wind velocity in Equation (9) and the amount of lift coefficient is about 1.2. Therefore, using 3D correction, lift coefficient improves by 14.1%. Finally, it shows that improvement in lift coefficient by 3D correction in such region that stall happens, could lead to achieving high improvement in prediction of normal force. When blade sits in upper half (azimuth angle between from 270˚ to 90˚), it is deeper into the wake than when it sits in bottom half. Therefore, normal force has a complicated trend and 3D correction can not have much improvement. This shows deep stall occurs at root span and upper half.

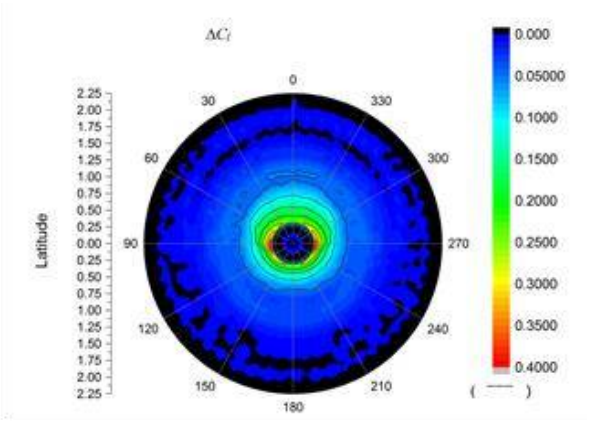

Figure 13. Distribution of ΔC_l on the rotor plan under yaw angle of 15◦.

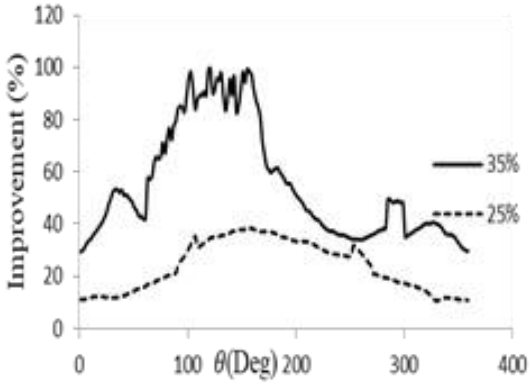

Figure 14. Percentage of improvement of the enhanced BEM model on normal force at 35% and 25% spans.

CONCLUSION

In this work, the BEM code was applied to simulate the MEXICO wind turbine project and assess the effect of 3D correction for the evaluation of normal force on the rotor blade at yaw condition. The characteristics of present work are summarized as follows:

1. Results show that the BEM code has good ability to predict the normal force in different sections of blade at yaw flow.
2. It is also found that the BEM calculation in the outer spanwise is more trustable than inner span wise (the radial distance more than 35% of the span).
3. The 3D correction does not affect improvement results at 60, 82 and 92% spans. It shows stall cannot happen and the advancing and retreating blade just can increase the cyclic loads in this sections.
4. Advancing and retreating blade cause deep stall by increasing the angle of attack at 25 and 35% spans.
5. It is found that the 3D correction has the maximum effect on 35% span at the azimuth angle between 60◦ to 183◦. By 3D correction, lift coefficient improves 14.1% and it leads to improve normal force about 99.57% at the azimuth angle 121◦.

REFERENCES

1. Khanjari, A., Sarreshtehdari, A. & Mahmoodi, E.2016. Modeling of Energy and Exergy Efficiencies of a Wind Turbine Based on the Blade Element Momentum Theory Under Different Roughness Intensities. J. Energy Resour. Technol. 139, 022006.
2. Mahmoodi, E. & Schaffarczyk, A. P. 2014. in 29–34 (Springer Berlin Heidelberg, 2014) .
3. Martinez, J., Bernabini, L., Probst, O. & Rodriguez, C. 2005. An improved BEM model for the power curve prediction of stall-regulated wind turbines. Wind Energy.
4. Vaz, J., Pinho, J. & Mesquita, A. 2011. An extension of BEM method applied to horizontal-axis wind turbine design. Renew. Energy .(2011)
5. Yang, H., Shen, W., Xu, H., Hong, Z. & Liu, C.2014. Prediction of the wind turbine performance by using BEM with airfoil data extracted from CFD. Renew. Energy 70, 107–115.
6. Mahmoodi, E., Jafari, A. & Keyhani, A. 2015. Wind Turbine Rotor Simulation via CTO Based Actuator Disc Technique Compared to Detailed Measurement. Int. J. Renew. Energy Dev. 4, 205–210.
7. Lanzafame, R., and M. M. 2012. How to take into account the radial flow inside of a 1-D numerical code. Renew. Energy 39 (1), 440–446.
8. Mahmoodi, E., Jafari, A., Peter Schaffarczyk, A., Keyhani, A. & Mahmoudi, J. 2013. A new correlation on the MEXICO experiment using a 3D enhanced blade element momentum technique. Int. J. Sustain. Energy 1–13
9. Li, Q., Kamada, Y., Maeda, T., Murata, J. & Yusuke, N.2016. Effect of turbulence on power performance of a Horizontal Axis Wind Turbine in yawed and no-yawed flow conditions. Energy 109, 703–711.
10. Bouatem, A. & Mers, A. Al. 2013. Validation of Chaviaro Poulos and Hansen Stall Delay Model in the Case of Horizontal Axis Wind Turbine Operating in Yaw Conditions. Energy Power Eng. 05, 18–25.
11. Schepers, J. & Snel, H. 2007. Model experiments in controlled conditions. ECN Rep. ECN-E-07-042. at <ftp://ftp.ecn.nl/pub/www/library/report/2007/e07042.pdf <
12. Schepers, J., Boorsma, K. & Snel, H. 2010. IEA Task 29 Mexnext: Analysis of wind tunnel measurements from the EU project Mexico. 3rd Torque 2010 Sci. Mak. Torque … 169–178.
13. Sørensen, J. 2011. Aerodynamic aspects of wind energy conversion. Annu. Rev. Fluid Mech. 427–448. 14. Glauert, H. Airplane propellers. Aerodyn. theory, 1935.
14. Hansen, A. & Butterfield, C. 1993. Aerodynamics of horizontal-axis wind turbines. Annu. Rev. Fluid Mech. 115–149.
15. Rankine, W. 1865. On the mechanical principles of the action of propellers. 13–39 .
16. Froude, W. 1878. On the elementary relation between pitch, slip and propulsive efficiency. 47–57
17. Froude, R. 1889. On the part played in propulsion by differences of fluid pressure. Trans. Inst. Nav. Archit. 390
18. Hernandez, J. & Crespo, A. 1987. Aerodynamics calculation of the performance of horizontal axis wind turbines and comparison with experimental results. Wind Eng 177–187
19. Moriarty, P. & Hansen, A. 2005. AeroDyn theory manual. at <http://www.nrel.gov/docs/fy05osti/36881.pdf<
20. Wilson, R. 2009.Wind Turbine Aerodynamics Part A: Basic Principles. … Wind Turbine Eng. Second.
21. Martinez, J., Bernabini, L., Probst, O. & Rodriguez, C. 2005. An improved BEM model for the power curve prediction of stall-regulated wind turbines. Wind Energy 385–402.
22. Snel, H., Houwink, R. & Bosschers, J. 1993. Sectional prediction of 3-D effects for stalled flow on rotating blades and comparison with measurements. 395–399.
23. P. K. Chaviaropoulos, Dr., 2000. Head of the Research and Development Department and M. O. L. Hansen, D. Investigating three-dimensional and rotational effects on wind turbine blades by means of a quasi-3D Navier-Stokes solver. J. Fluids Eng. 122.
24. Breton, S. 2008. Study of the stall delay phenomenon and of wind turbine blade dynamics using numerical approaches and NREL's wind tunnel tests. Dr. theses NTNU
25. Schepers, J. G. et al. 2012. Final report of IEA Task 29, Mexnext (Phase 1): Analysis of Mexico wind tunnel measurements. 312.
26. Schepers, J. 1998. An engineering model for yawed conditions, developed on the basis of wind tunnel measurements .
27. Micallef, D., Van Bussel, G., Ferreira, C. S. & Sant, T. 2013. An investigation of radial velocities for a horizontal axis wind turbine in axial and yawed flows. Wind Energy 16.

Persian Abstract

DOI: 10.5829/ijee.2018.09.01.03

چکیده

در این مقاله اثر تاخیر واماندگی بر روی توزیع نیروی محوری وارده به مقاطع مختلف پره توربین بادی به وسیله نظریه ارتقاء یافته تکانه اجزاء پره و همچنین با در نظر گرفتن ضریب اصلاح سه بعدی ایرفویل چاویروپلوس و هانسن صورت گرفت. نتایج به دست آمده با مقادیر اندازه¬گیری شده در سرعت باد ۲۴ متر بر ثانیه و زاویه یاو ۱۵ درجه مورد مقایسه قرار گرفتند. نتایج نشان داد که مقادیر محاسبه شده در مقاطع بیرونی تر پره توربین بادی قابل اعتمادتر هستند نسبت به مقاطع نزدیک به ریشه پره. در مقاطع بیرونی ٪۶۰، ٪۸۲ و ٪۹۲ ضریب تصحیح سه بعدی استفاده شده اثر قابل لمسی بر بهبود نتایج نداشت که به معنی عدم رخداد پدیده واماندگی است. در قسمت های میانی پره ٪۲۵ و ٪۳۵ سرعت باد به مقدار فزاینده ای افزایش یافت و به طبع آن زاویه حمله نیز افزایش یافت و با عث وقوع واماندگی شد. که در این ناحیه¬ها اثر ضریب سه بعدی به وضوع مشاهده شد. بیشترین بهبود توسط این ضریب در مقطع ٪۳۵ و در زاویه صفحه ۱۲۱ درجه به مقدار ٪۹۵/۵۷ بود